

RESEARCH

Open Access



Design of passive suspension system to mimic fuzzy logic control active suspension system

Mahesh Nagarkar^{1*}, Yogesh Bhalerao^{2,3}, Dhiraj Bhaskar¹, Ajaykumar Thakur¹, Vaibhav Hase⁴ and Rahul Zaware⁵

Abstract

Background: This paper proposes a method for designing a passive suspension system that determines the optimal suspension settings while offering feasible performance near an active suspension system. A mathematical model of a nonlinear quarter car is developed and simulated for control and optimization in MATLAB/Simulink[®] environment. The input road condition is a Class C Road, and the vehicle moves at 80 kmph. Fuzzy logic control (FLC) action is used to accomplish active suspension system control. An approach for investigating optimal suspension settings based on the FLC control force is described here. The optimized passive suspension system is supposed to have the same suspension travel and velocity as an active suspension system. The least square technique is implemented to optimize the suspension parameters of the passive suspension system.

Results: The initial passive suspension system, FLC active system, and optimized suspension system are simulated in MATLAB/Simulink[®] environment. It is observed that RMS acceleration for the FLC system is 0.5057 m/s², which is reduced by 46% (passive suspension system has RMS acceleration of 0.9322 m/s², which is uncomfortable). For optimized system, RMS acceleration is 0.6990 m/s². It is observed that the optimized passive suspension system almost mimics the initial FLC active suspension system. For the optimized system, sprung mass acceleration and VDV are improved by 30% and 27%, respectively, compared to the initial passive system.

Conclusion: It is observed that the optimized passive suspension system mimics the initial FLC system. Also, an optimized FLC system has improved health criterion-based results compared to other suspension systems.

Keywords: Health criterion, Nonlinear suspension system, Fuzzy logic control, Optimization, Mimic

1 Background

Automobile suspension systems isolate passengers from shock and vibrations caused by uneven road surfaces. As a result, the suspension system improves ride comfort, reduces driver fatigue, and improves driver health and safety. A suspension system's other performance criteria include successfully supporting the vehicle's weight, keeping the wheels in the appropriate position for better

handling, and keeping the tire in contact with the ground. A passive suspension system has to achieve a trade-off between ride comfort and handling [1]. Many researchers have investigated the suspension system because of the competing criteria to find the best compromise between the competing requirements. Researchers have studied the optimization of vehicle suspension systems using various vehicle and suspension models to find optimal suspension parameters among the conflicting requirements. Gobbi and Mastinu [2] implemented a 2-DoF quarter car model traversing on a random road profile to optimize the suspension system using discomfort, suspension working space, and holding as objective criteria. An optimization method based on multi-objective programming

*Correspondence: maheshnagarkar@rediffmail.com

¹ Department of Mechanical Engineering, Sanjivani College of Engineering, Koprgaon, Savitribai Phule Pune University, Pune 423603, India
Full list of author information is available at the end of the article

and monotonicity is implemented to derive optimal parameters, symbolically or numerically, such as spring and tire stiffness and damping. Authors have derived the optimal suspension parameters using 1D and 2D PSD road surfaces and obtained better comfort, suspension space, and road holding, whereas the tire stiffness is always kept at a lower value. Özcan et al. [3] have optimized light vehicles used for commercial purposes for comfort and handling. MATLAB/Simulink® environment is used to simulate quarter car and half-car models. The Carmaker® model is used to validate the performance of an optimized suspension system. Authors have obtained time domain results of RMS body acceleration, tire forces, and RMS body roll using MATLAB/Simulink and Car Maker. It is observed that optimized parameters have improved time domain results compared to initial suspension parameters. An advantage of nonlinear suspension over initial suspension was observed with the Carmaker model through the double lane change technique maneuvering. Chi et al. [4] employed a genetic algorithm (GA), pattern search algorithm (PSA), and sequential quadratic programming (SQP) to optimize the linear suspension system. Authors have used body acceleration, rattle space, and tire load as optimization criteria. It is found that GA and PAS are more reliable than SQP algorithms. Authors have selected sprung and unsprung mass, suspension, tire stiffness, and suspension damping as design variables, whereas body acceleration, suspension space, and tire force are the objective functions. Authors have optimized the suspension parameters for various road surfaces and speeds and obtained optimal results. The particle swarm optimization technique is used by Gomes [5] to optimize a quarter car model traveling over a random road profile. The author used rattle space and dynamic load as the optimization criterion. The authors have presented two examples—dynamic load due to suspension and suspension deflection. The first case yields better results compared to the initial one. It is observed that the suspension and tire stiffness converged to upper and lower bounds, whereas suspension damping converged to the upper bound. Baumal et al. [6] implemented a half-car model to search the design parameters of a half-car model using a genetic algorithm. Minimizing passenger seat acceleration is the optimization objective with road holding and rattle space as constraints. The results of GA are compared with the gradient projection method and observed that GA yields better results. The GA results may be further improved by fine-tuned population size and mutation; however, authors have observed that GA requires more computing efforts. Kuznetsov et al. [7] implemented optimization of 3-DoF driver car model (1-DoF driver coupled with a 2-DoF quarter car) using ISO 2631-1-based ride comfort with the algorithm

for a global optimization problems (AGOP). Authors have obtained the numerical results on actual road data of three surfaces with two design scenarios—with human and without human models. It is observed that optimized suspension parameters significantly affected ride comfort at high speed, whereas the overall damping coefficient has a notable impact on ride comfort in both scenarios. Optimization of quarter car model with 2-DoF driver model was presented by Gundogdu [8]. A multi-objective problem, consisting of head acceleration, crest factor, rattle space, and tire deformation objectives, converted into a uni-objective problem with non-dimensional expressions and implemented using GA. The author used step as input road condition, whereas time and frequency domain results are obtained for head, pelvis, and thorax force. The optimized results are less oscillatory, better ride comfort and stability, and lower crest factor (CF) and VDV values. The author concluded that while optimizing the suspension system, one should include ride and health criteria which includes head acceleration, CF, and VDV. The above literature shows that a vehicle model is optimized using various optimization algorithms with or without a driver model.

The purpose of an active suspension system is to replace traditional passive elements with a controlled system that can deliver force to the system. Because of its ability to supply energy to achieve relative motion between the body and wheel, active suspension systems dynamically respond to changing road surfaces, improving various performance criteria such as ride comfort, body displacement, suspension space requirements, and tire forces, among others. For active control, researchers employed different control methods such as robust control, nonlinear control, nonlinear backstepping control, PID control, PI sliding mode control, Fuzzy logic control, and so on. One of the primary goals was to reduce body acceleration to enhance ride comfort [9–13]. The author discussed various vehicle models such as simple 1 DoF, quarter car, half car, and full car models. The author studied the advancements in optimal controller design, its use for ride comfort, and vehicle stability applied to simple and complex vehicle models [9, 10], whereas [11] introduced LQR and backstepping control algorithm for ride comfort. It is observed that both methods yield the same results, and the ride comfort is better compared to a passive suspension system. Authors have concluded that the ability of controllers to adapt to uneven road surfaces is the real challenge. Authors [12] have studied PID and LQR controllers on a nonlinear quarter car model. The controller parameters such as ride comfort, health, and stability are optimized using GA techniques, and results are compared with a passive suspension system. It is observed that PID controllers yield better results in terms

of ride comfort, health criterion, and vehicle stability. A PI sliding mode controller is presented by [13] implemented on a quarter car. The authors concluded that the PI sliding mode controller performs better and is more robust than the LQR and passive systems.

This research proposes an approach for designing passive suspension parameters using the FLC active suspension system. FLC-based active suspension systems are commonly used to control the suspension system. A fuzzy logic-based active quarter car suspension system was investigated by Kalaivani et al. A hybrid differential evolution-based biogeography-based optimization algorithm is used to tune the scaling factors of the FLC controller. RMS body acceleration is used as an objective function to optimize PID and FLC controller parameters. The FLC controller performs better than the PID controller and passive system regarding suspension acceleration, rattle space, and tire deflection. Frequency and time domain results are presented to show the effectiveness of the proposed controller [14]. The FLC controller was implemented on a quarter car test rig by Taskin et al. and studied FLC controller to improve ride comfort. Body velocity and suspension deflection were input to the controller, whereas controller force is the output. From the time response of the FLC active system, it is observed that body displacement is minimized without losing suspension working space. Results were also obtained in the frequency domain, which shows improved ride comfort [15]. Huang and Chao implemented a fuzzy logic controller-based active suspension system on a quarter automobile model. A quarter car model was implemented for the suspension study. Tire deformation plays a significant role in the control performance of the active suspension system; hence, tire deformation is predicted using a gray predictor. Results showed that the control strategy improves ride comfort by reducing body oscillations [16]. Salem and Aly had researched the 2-DoF quarter suspension system. The FLC was applied to control the quarter car active suspension system. Body acceleration was used as a criterion to study the ride comfort of a suspension system with handling. FLC and PID controllers were investigated, and FLC performs better [17]. According to the previous discussions, researchers [15–17] have successfully implemented the FLC for ride control applications, whereas [14] improved the FLC using a single optimization function.

Ding et al. [18] observed that traditional fuzzy PID controller has limitations in adapting according to the road surface. The authors had studied multiple fuzzy PID controllers in which the varying road conditions were taken care of by secondary adjustment of PID control parameters. Authors have implemented this strategy on a quarter car model with road prediction by neural

networks. The sprung mass acceleration was studied, and the acceleration was observed to be lower than a passive and conventional fuzzy PID controller. Experimental results showed better performance of the controller. Nasir [19] presented active control methods for the vehicle suspension system and implemented LQR, H2, PID, and FLC with the GA technique. It was observed that H2 satisfies maximum overshoot, whereas settling time was out of requirements. PID and LQR methods need more controller parameter tuning to achieve desired results. In contrast, GA-PID and GA-FLC achieved maximum overshoot and desired settling time while showing better performance. Thus, GA tuned controller offered better ride comfort over H2 and LQR.

Senthilkumar et al. [20] studied a full car model with 7 DoF for ride and control applications. The authors observed body displacement and acceleration for FLC, PID controller, and passive system. It is observed that the FLC has better performance offering better ride comfort and resonance peak due to the body acceleration being decreased compared to PID and passive systems. Basari et al. [21] presented the FLC of the half-car model in a MATLAB/Simulink® environment and compared it with a passive suspension system. The body acceleration and wheel deflection were the output parameters to test the performance of the suspension system. A single road bump was the input to both tires, and results are presented in the time domain only. It is observed that the FLC active system had less settling time and body acceleration. Thus, FLC active system offers better ride comfort. Likaj et al. [22] presented active control of the quarter car system using LQR and FLC strategies. The ride comfort of the vehicle had studied with the help of body displacement and acceleration. It is observed that FLC shows better results as compared to the LQR controller in terms of body displacement and acceleration. Rajendiran and Lakshmi [23] analyzed active control of 2 DoF suspension systems using PID control and FLC along with the seat and driver model. Authors have derived an 8-DoF integrated driver-vehicle model and simulated it for four road models—single bump, double bump, sine wave, and random road profile. The authors observed head acceleration and controller force to test the efficacy of the controller. It is observed that FLC improves ride comfort more than that PID control and passive system for all four road profiles.

The data for this investigation are taken from a work by Nagarkar et al. [24], in which authors presented the modeling of a nonlinear quarter car model and its control using FLC and PID controllers. The controller parameters, such as PID parameters such as P, I, D, and FLC range of input and output membership function and scaling factors, are optimized in the MATLAB/Simulink

environment using the NSGA-II algorithm. These controller parameters are tailored for vibration dose value (VDV), frequency-weighted RMS acceleration, RMS rattle space, RMS tire deflection, and RMS control force, among other objective functions. ISO 2631-1 approach is implemented to determine the objective functions, and results are obtained in time and frequency domains. It has been discovered that an optimized FLC outperforms a PID and a passive suspension system.

The FLC active suspension system is used to design the parameters of the passive suspension system. The passive system is first modeled and simulated to determine the suspension force with FLC [24]. The suspension force is equal to the sum of the spring-damper force and the actuator force when the FLC action is used. The optimized passive suspension system is assumed to have the same suspension travel and velocity as an active suspension system. Thus, the spring-damper force of the optimized passive system is the same as that of the active system. The optimized parameters are tested based on health criteria using Annexure B of ISO 2631-1 [25].

This paper uses a computationally simple method to obtain optimal suspension parameters. The advantages of this technique are that—

- Computationally simple and requires less computation time.
- It does not require a complex optimization algorithm.
- Do not require any algorithm-specific parameters.
- Yields results as close to the active suspension system.
- This method can be employed for any controller.

But the limitation is that this method needs a controller for time histories from the active suspension system.

2 Methods

2.1 Mathematical modeling of nonlinear quarter car suspension system

For control and optimization applications, a nonlinear quarter car suspension model [24, 26] is utilized. In this study, a quarter car is modeled as a nonlinearity with quadratic tire stiffness and cubic stiffness in the suspension spring, as illustrated in Fig. 1.

The governing equations of the system are defined as—

$$\left. \begin{aligned} m_{us}\ddot{x}_{us} - c_s(\dot{x}_s - \dot{x}_{us}) - k_s(x_s - x_{us}) + k_{tnl}(x_{us} - x_r)^2 - k_{snl}(x_s - x_{us})^3 + k_t(x_{us} - x_r) - f_{flc} &= 0 \\ m_s\ddot{x}_s + c_s(\dot{x}_s - \dot{x}_{us}) + k_s(x_s - x_{us}) + k_{snl}(x_s - x_{us})^3 + f_{flc} &= 0 \end{aligned} \right\} \quad (1)$$

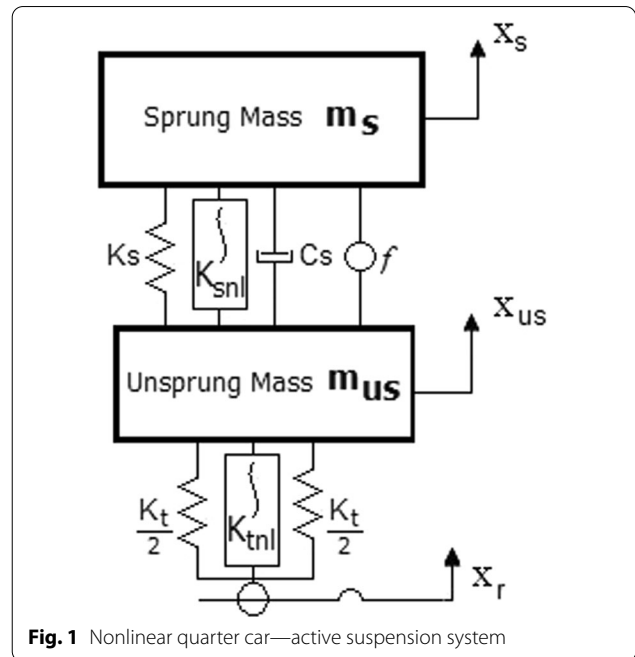


Fig. 1 Nonlinear quarter car—active suspension system

2.2 Fuzzy logic control of nonlinear quarter car

FLC is a heuristic-based human-in-loop control that uses rule-based information obtained from user experience [14–16]. Figure 2 represents a typical FLC structure with a 2-DoF quarter car. FLC has two inputs—sprung mass velocity and acceleration, and FLC force is the output.

In this study [24], FLC consists of seven membership functions each, for two inputs and an output with Mamdani fuzzy inference system and centroid defuzzification method. The FLC controller is optimized using the NSGA-II [27] algorithm having objective functions such as frequency-weighted RMS acceleration, VDV, RMS suspension travel, RMS tire deflection, and RMS control force. The design variables are scaling factors of input and output and the range of membership functions [24]. The rule base of the FLC force is represented in Fig. 3.

The critical decision in optimization problems is to select proper objective functions. The FLC is implemented to improve ride characterized by RMS frequency-weighted sprung mass acceleration, VDV, RMS suspension space deflection, RMS tire deflection, and

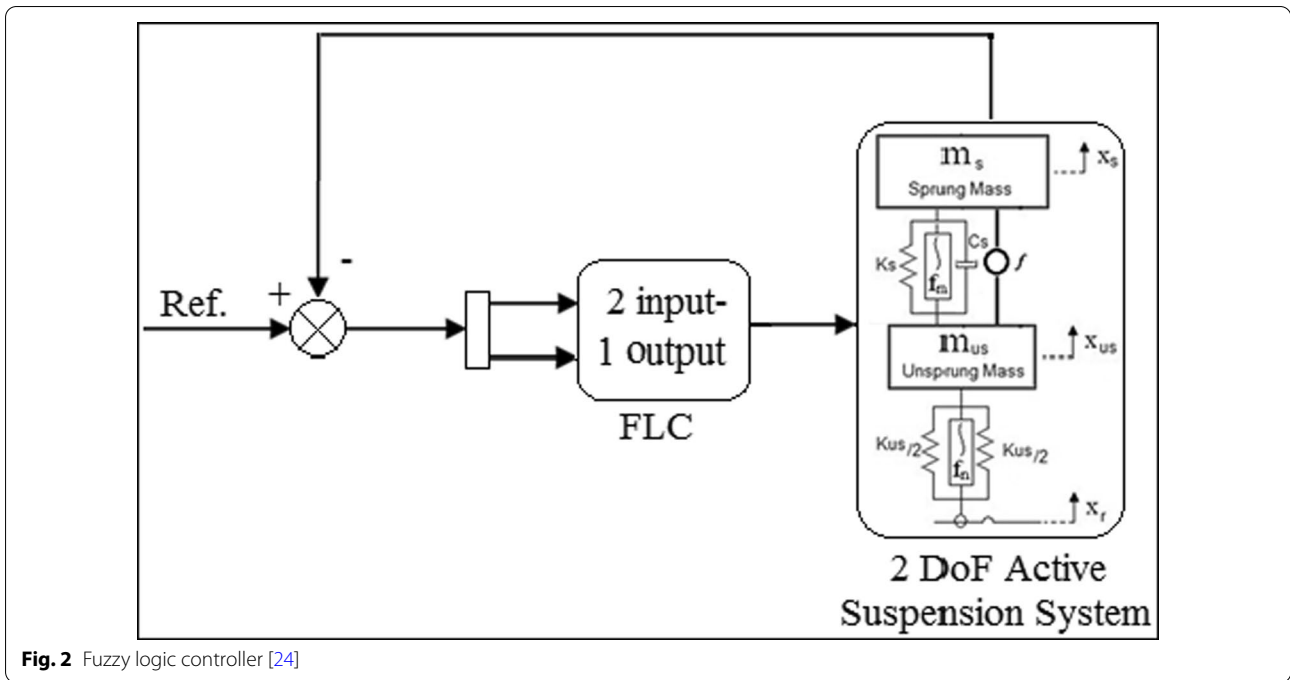


Fig. 2 Fuzzy logic controller [24]

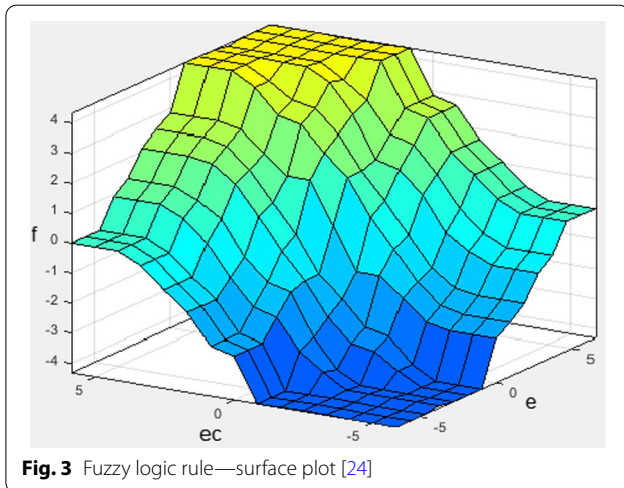


Fig. 3 Fuzzy logic rule—surface plot [24]

RMS controller force. The objective functions are defined as follows—

Frequency-weighted RMS acceleration As per ISO 2631-1 (1997), RMS acceleration is given by

$$A_w = \left\{ \frac{1}{T} \int_0^T [a_s(t)]^2 dt \right\}^{\frac{1}{2}} \tag{2}$$

According to ISO 2631-1 (1997), VDV assesses the cumulative effect of vibrations on the body; thus, it is a measure for whole body vibrations.

Vibration dose value (VDV) VDV is the fourth power of acceleration time histories. It is expressed by Eq. (3)—

$$VDV = \left\{ \int_0^T [a_w(t)]^4 dt \right\}^{\frac{1}{4}} \tag{3}$$

Suspension travel Suspension travel is characterized by the relative travel between the sprung and unsprung mass.

$$RMS \text{ Suspension Travel} = \left\{ \frac{1}{T} \int_0^T [(x_s(t) - x_{us}(t))]^2 dt \right\}^{\frac{1}{2}} \tag{4}$$

Dynamic tire deflection Dynamic tire force is related to tire deflection. The following equation expresses the RMS of tire deflection—

$$RMS \text{ Tire Deflection} = \left\{ \frac{1}{T} \int_0^T [(x_{us}(t) - x_r(t))]^2 dt \right\}^{\frac{1}{2}} \tag{5}$$

Control force is introduced as one of the objective functions to find the optimum control force to achieve ride comfort.

$$RMSf = \left\{ \frac{1}{T} \int_0^T [(f_{FLC}(t))]^2 dt \right\}^{\frac{1}{2}} \tag{6}$$

2.2.1 Optimization of fuzzy logic control using NSGA-II algorithm

FLC with 2 input–1 output functions is initialized with trapezoidal membership functions having range $[-1, 1]$ and is multiplied with scaling factors. Also, inputs sprung mass velocity (error, e), mass acceleration (change in error, ec), and control output (f) are scaled using scaling factors ke , kec , and kf , respectively. The search space for the input–output membership functions and scaling factors is

- Membership Functions for Input 1 $\in [1, 10]$,
- Membership Functions for Input 2 $\in [1, 10]$,
- Membership Functions for Output $\in [1, 10]$,
- $ke \in [-5, 5]$, $kec \in [-5, 5]$, $kf \in [0, 25]$ [18]

The FLC is optimized by implementing the objective functions represented by Eqs. (2)–(7) and the search spaces defined above for the design variables. The optimized values are then further implemented using MATLAB/Simulink® and the quarter car model, and time domain results are obtained.

The optimization problem involves objectives such as ride comfort, health criterion, and stability; thus, problem becomes multi-objective optimization (MOO). The MOO problem consists of multiple solutions, thus forming a Pareto-front. NSGA-II is implemented [24] due to the ability of an algorithm to handle multi-domains as it handles noisy and multi-modal complex and discontinues functions. NSGA-II supports parallel computing, and a non-dominated sorting algorithm reduces computing complexities. NSGA-II supports diversity by crowding distance and uniform spread operators [27]. Figure 4 represents the flowchart of the NSGA-II algorithm.

2.3 Optimization of passive suspension system to mimic FLC

In this study, optimization of passive suspension to mimic the FLC active suspension system is implemented by incorporating results obtained by Nagarkar et al. [24]. An NSGA-II algorithm is used to optimize the controller parameters for optimal results [24]. As a result, the suspension system is optimized to mimic the active control system, and outcomes of the NSGA-II optimized FLC are implemented. The FLC active suspension system is designed to minimize the objective functions such as RMS f_{flc} , VDV, frequency-weighted RMS acceleration, RMS suspension travel, and RMS tire deflection.

The passive suspension system under optimization study is considered to have the same suspension travel and velocity as an active suspension system. The actuator force generated by FLC active system is deemed equal

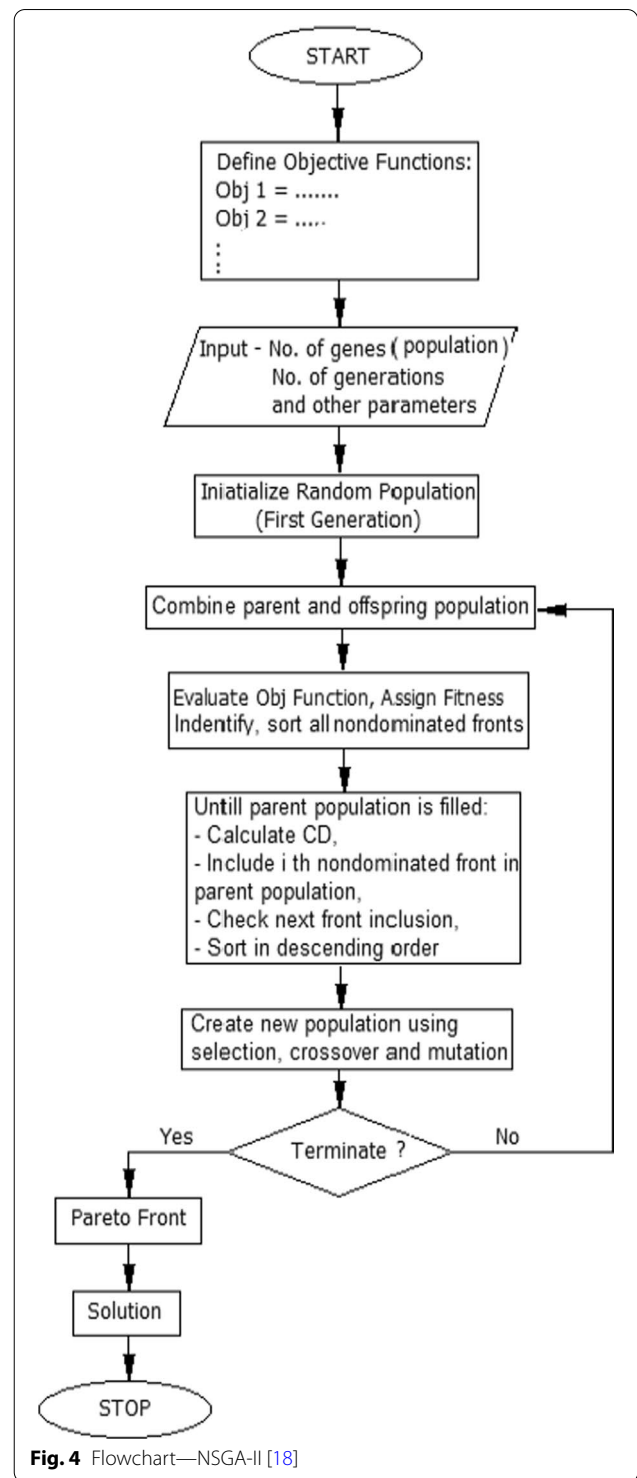
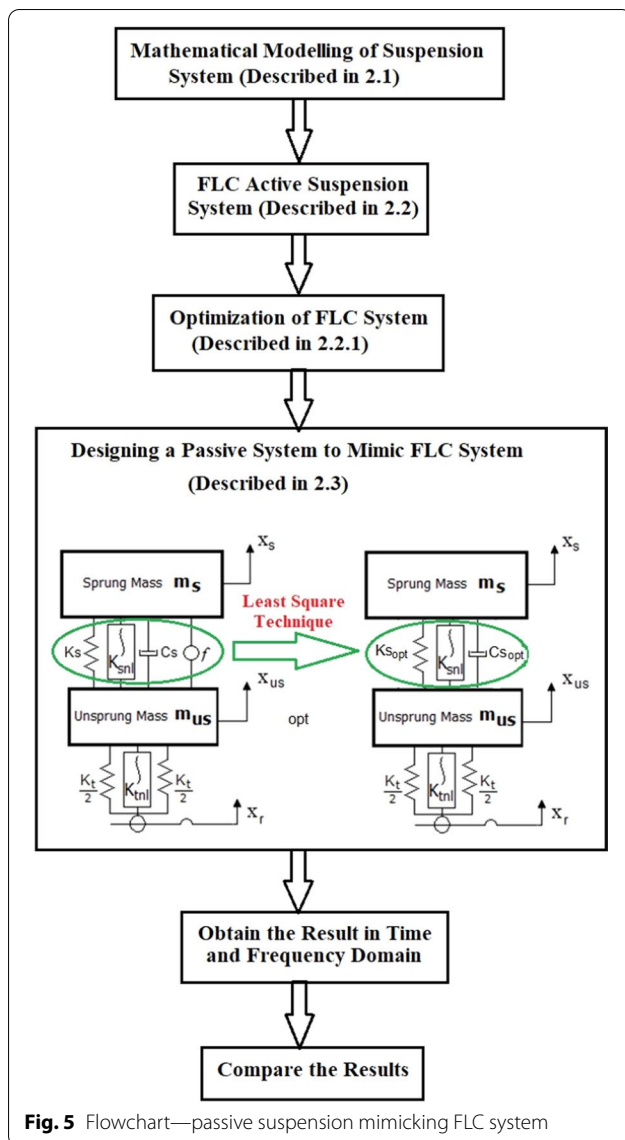


Fig. 4 Flowchart—NSGA-II [18]

to spring and damper forces generated by the initial passive suspension system. The methodology is explained in Fig. 5.



As a result, Eq. (7) gives the generated suspension force for the passive system as follows:

$$f_p = k_s(x_s - x_{us}) + c_s(\dot{x}_s - \dot{x}_{us}) + k_{snl}(x_s - x_{us})^3 \quad (7)$$

Let x_1 be suspension travel and \dot{x}_1 be suspension velocity, Eq. (7) becomes

$$f_p = k_s(x_1) + c_s(\dot{x}_1) + k_{snl}(x_1)^3 \quad (8)$$

In an active system using FLC, the input control force is f_{flc} . The optimal parameters of a passive suspension system are obtained by the least square technique, where a square of force error is minimized, i.e.,

$$\min_{k_s, c_s} \sum_t [f_{flc}(t) - f_p(t)]^2 \quad (9)$$

Partially differentiating Eq. (9) with respect to k_s and c_s and equating it to zero to obtain optimal suspension parameters. Thus, for optimal k_s and c_s we have

$$\frac{\partial}{\partial k_s} \sum_t [f_{flc}(t) - f_p(t)]^2 |_{k_s=k_{sopt}} = 0 \quad (10)$$

$$\frac{\partial}{\partial c_s} \sum_t [f_{flc}(t) - f_p(t)]^2 |_{c_s=c_{sopt}} = 0 \quad (11)$$

Solving Eqs. (10) and (11) by substituting f_p from Eq. (3), we have

$$k_{sopt} \sum (x_1)^2 + c_{sopt} \sum [(\dot{x}_1).(x_1)] = \sum [f_{flc}.(x_1)] - k_{snl} \sum (x_1)^4 \quad (12)$$

and

$$k_{sopt} \sum [(\dot{x}_1).(\dot{x}_1)] + c_{sopt} \sum (\dot{x}_1)^2 = \sum [f_{flc}.\dot{x}_1] - k_{snl} \sum [(\dot{x}_1).(x_1)^3] \quad (13)$$

Rearranging Eqs. (12) and (13) in matrix form,

$$\begin{bmatrix} \sum (x_1)^2 & \sum [(\dot{x}_1).(x_1)] \\ \sum [(\dot{x}_1).(x_1)] & \sum (\dot{x}_1)^2 \end{bmatrix} \begin{Bmatrix} k_{sopt} \\ c_{sopt} \end{Bmatrix} = \begin{bmatrix} \sum [f_{flc}.(x_1)] - k_{snl} \sum (x_1)^4 \\ \sum [f_{flc}.\dot{x}_1] - k_{snl} \sum [(\dot{x}_1).(x_1)^3] \end{bmatrix} \quad (14)$$

Thus, we have

$$\begin{Bmatrix} k_{sopt} \\ c_{sopt} \end{Bmatrix} = \begin{bmatrix} \sum (x_1)^2 & \sum [(\dot{x}_1).(x_1)] \\ \sum [(\dot{x}_1).(x_1)] & \sum (\dot{x}_1)^2 \end{bmatrix}^{-1} \begin{bmatrix} \sum [f_{flc}.(x_1)] - k_{snl} \sum (x_1)^4 \\ \sum [f_{flc}.\dot{x}_1] - k_{snl} \sum [(\dot{x}_1).(x_1)^3] \end{bmatrix} \quad (15)$$

3 Results

The suspension parameters in [24] simulate a nonlinear quarter car model described by Eq. (1) in the MATLAB/Simulink® environment. The input road condition is modeled as a class C road (average road) with $512 \times 10^{-6} \text{ m}^2/(\text{cycle}/\text{m})$ of road roughness [28]. The vehicle is traveling at an average speed of 80 kmph. The class C road surface is depicted in Fig. 6.

The suspension system is then simulated for ride and control applications in MATLAB/Simulink environment, and the results obtained by Nagarkar et al. [18] are implemented in this paper.

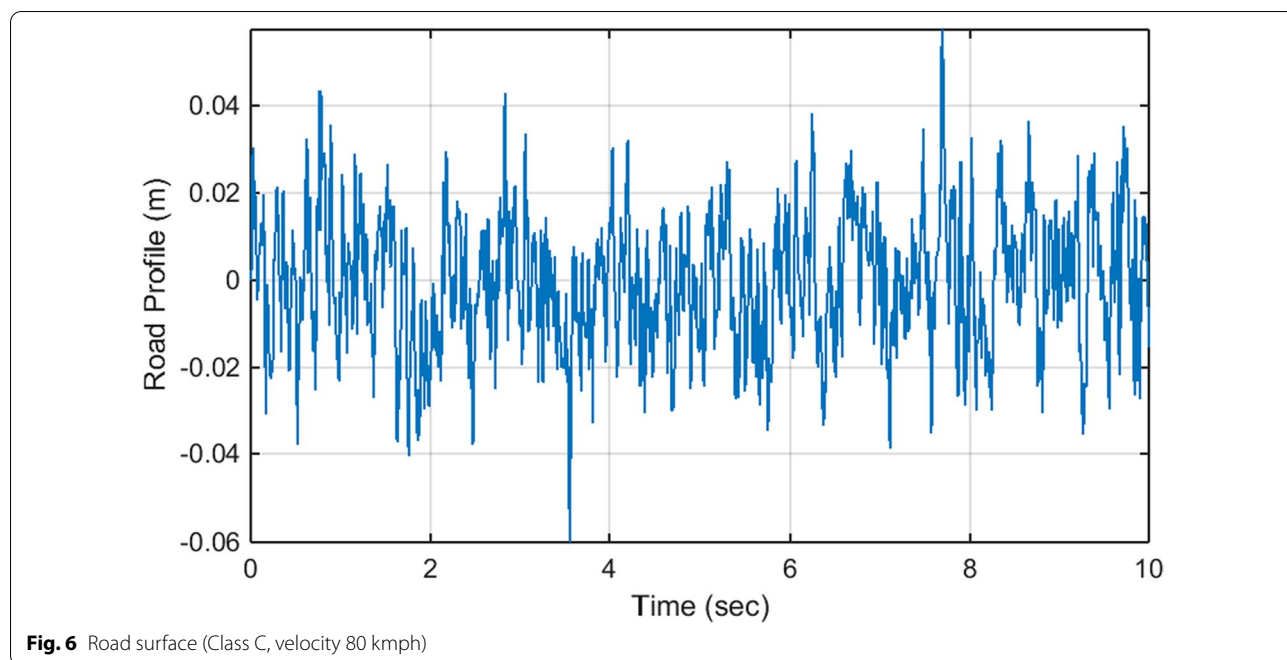


Fig. 6 Road surface (Class C, velocity 80 kmph)

Table 1 Optimized suspension parameters

Suspension parameters	K_s	c_s
Value	12,523.0861	314.2430

Authors [24] have used frequency-weighted RMS acceleration, VDV, RMS suspension space, RMS tire deformation, and RMS controller force as the objective function to optimize the range of membership functions of the FLC and scaling factors. For detailed analysis, please refer to [24].

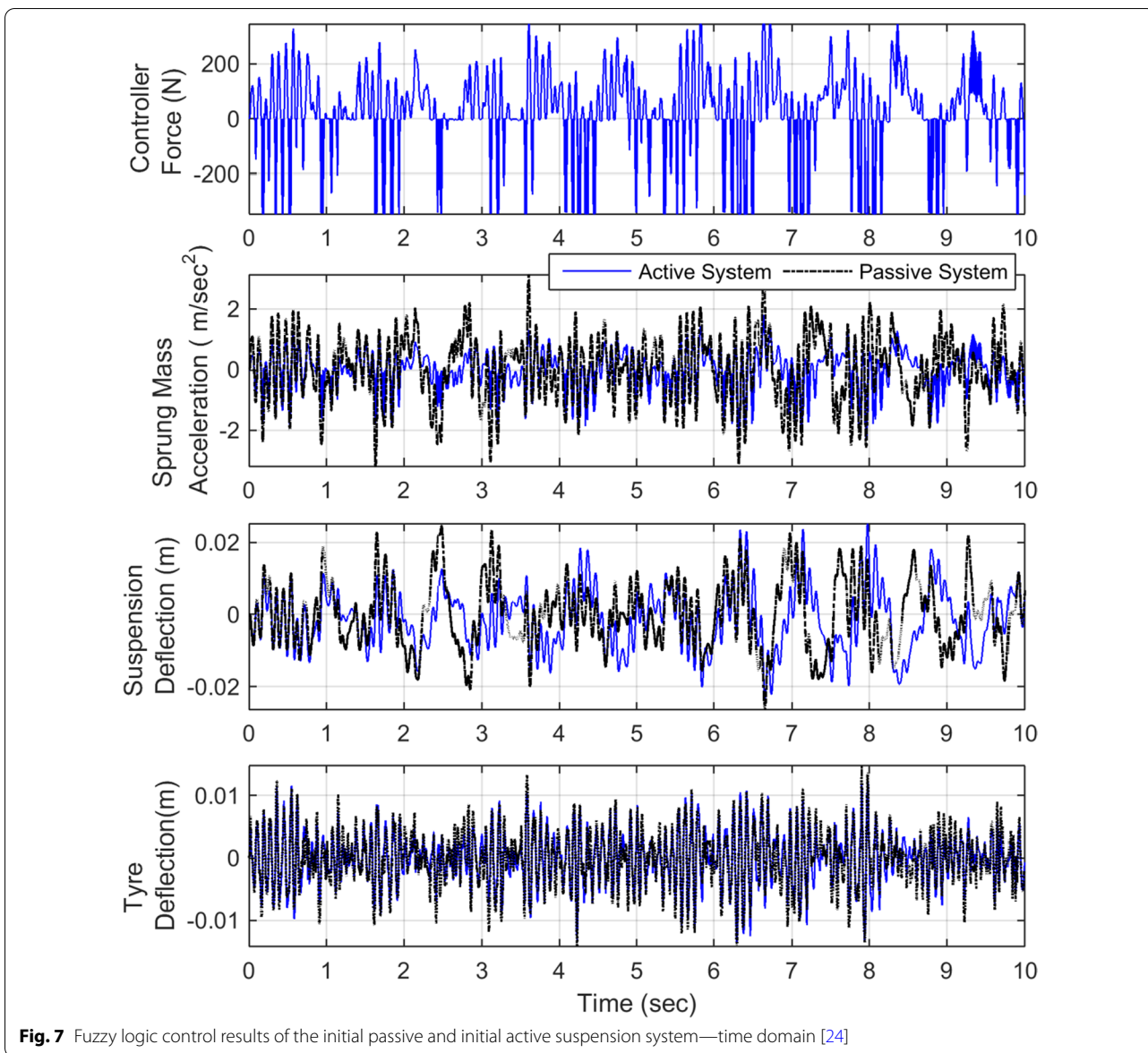
The simulation for the control on the 2-DOF non-linear suspension system is excited by a random road

disturbance, as shown in Fig. 6. The FLC control force, suspension travel, and velocity signals are obtained from [24]. The initial passive suspension system is optimized using FLC results from [24] and Eq. (15). The optimized suspension parameters which mimic the FLC suspension system are given in Table 1.

Various output parameters, such as controller force, VDV, and frequency-weighted RMS acceleration, are obtained and represented in Table 2. Time domain results are shown in Fig. 7 for the initial passive and FLC active system. Figure 8 shows time domain plots of the FLC active suspension system and passive suspension system, which mimics the FLC system with optimized parameters, whereas Fig. 9 represents error signal

Table 2 FLC and passive suspension system results

Parameters	Initial suspension system		Optimized suspension system	
	Passive system	FLC system	Passive system	FLC system
Control force (N)	–	140.9662	–	86.4596
VDV ($m/s^{2.75}$)	2.1509	1.1782	1.5511	0.8005
Frequency-weighted RMS acceleration (m/s^2)	0.9322	0.5057	0.6474	0.3606
RMS suspension space deflection (m)	0.009311	0.0085	0.01215	0.009866
RMS tire deflection (m)	0.004473	0.0042	0.007275	0.007013
Max control force (N)	–	345.6605	–	345.6605
Max acceleration (m/s^2)	3.16720	2.31900	2.9985	1.7594
Max suspension space deflection (m)	0.02640	0.02520	0.04487	0.03029
Max tire deflection (m)	0.01840	0.01350	0.0235	0.02097



plots, and Fig. 10 shows a combined plot of initial passive, optimized passive system, and FLC systems with initial suspension parameters and optimized suspension parameters.

Moreover, to validate the performance of these four types of systems, frequency domain plots are shown in Fig. 11 and Table 3.

The health risk associated with the magnitude and vibration duration exposure is assessed using the Health Guidance Caution Zone (HGCZ) described in Annexure B of ISO2631-1. The frequency-weighted RMS acceleration criterion is used in this study to evaluate the amplitude and duration of vibration exposure. This criterion is used to predict health risk and is divided into three

primary levels of exposure: no health risk (NHR), potential health risk (PHR), and likely health risk (LHR), as shown in Fig. 12. NHR, PHR, and LHR limit values for time duration are shown in Table 4.

4 Discussion

The suspension system is then simulated using optimized parameters as listed in Table 1. The results for the initial passive suspension system and the FLC active suspension system are listed in Table 2 and presented in Fig. 7. The RMS acceleration for fuzzy logic control is found to be 0.5057 m/s^2 , which is a little uncomfortable. RMS acceleration is lowered by 46% (passive suspension has the RMS acceleration of 0.9322 m/s^2 , which is

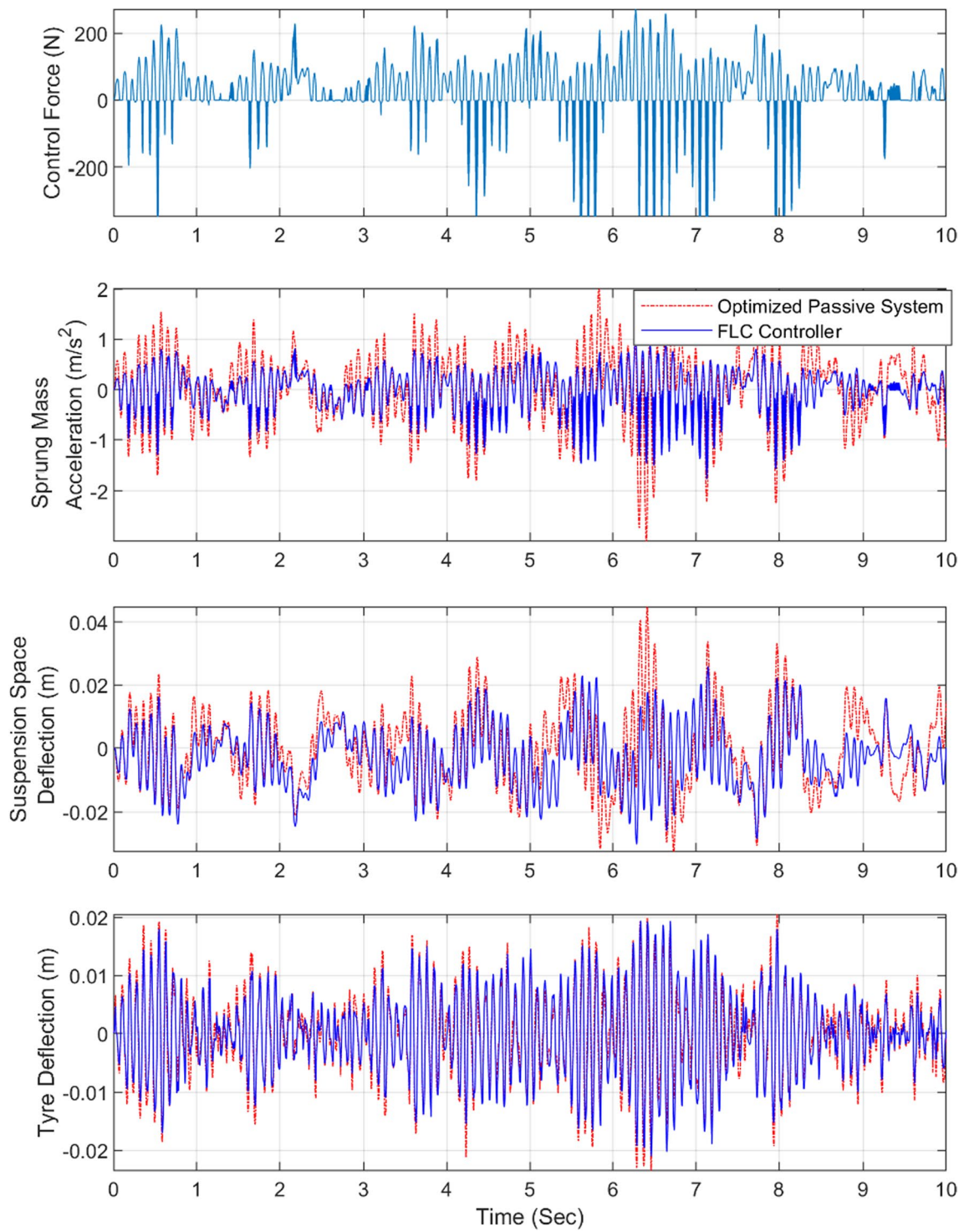


Fig. 8 Time domain results—optimized passive and initial FLC suspension system

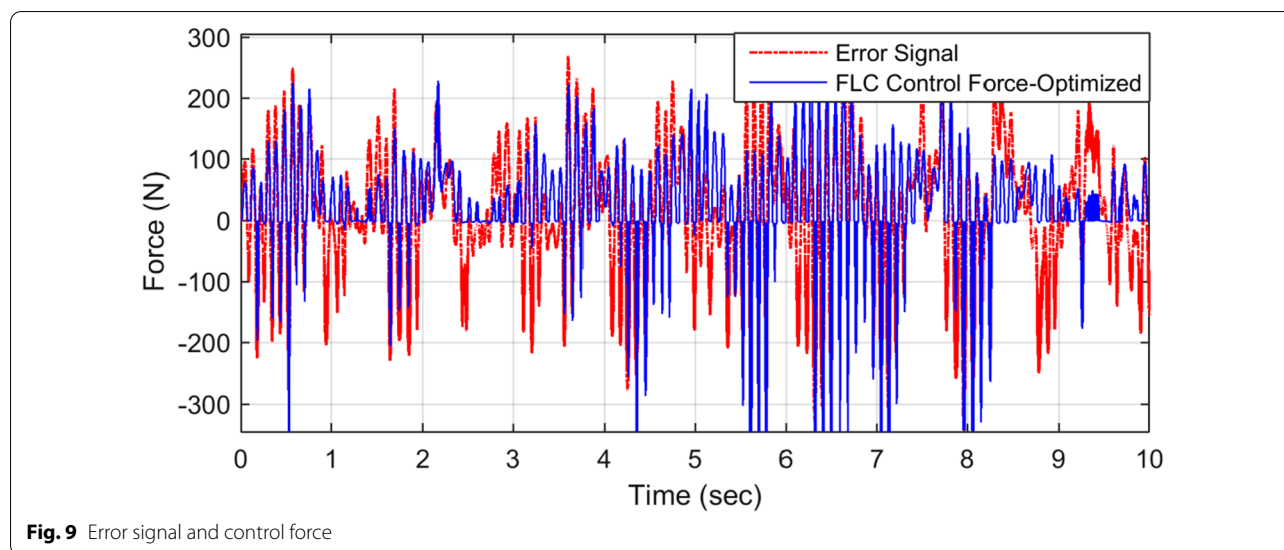


Fig. 9 Error signal and control force

uncomfortable), and VDV is reduced by 45% in the fuzzy logic control system compared to the passive suspension system. In addition, when compared to a passive suspension system, RMS suspension space and RMS tire deflection are lower. Table 2 also includes the results of RMS optimal control force, RMS sprung mass acceleration, RMS suspension space, dynamic tire force, road holding, maximum controller force, and maximum sprung mass acceleration.

In a MATLAB/Simulink environment, an optimized passive suspension system is simulated and compared to the initial FLC suspension system. Figure 8 depicts the findings of the time history analysis. Table 2 lists the RMS acceleration VDV and other results. The time history findings of sprung mass acceleration, suspension space, and tire deflection for FLC and optimized passive suspension systems are virtually identical. Refer to Fig. 8. As a result, the optimized passive suspension system appears similar to the FLC suspension system.

Compared to the initial passive suspension system, which has the RMS acceleration of 00.9322 m/s^2 , which is uncomfortable, the optimized passive suspension system has the RMS acceleration of 0.6474 m/s^2 , which is a little uncomfortable. Furthermore, compared to the initial passive suspension system, the RMS acceleration of the optimized passive suspension system is 30% lower. In addition, compared to the initial passive suspension system, the VDV of the optimized passive suspension system is 27% lower. Hence, compared to the initial passive suspension system, the optimized passive suspension system improves ride comfort and nearly mimics the initial FLC active suspension system.

Further, an error signal, the difference between FLC force and initial passive suspension force, is obtained in

MATLAB/Simulink environment. Figure 9 represents the plot of the error signal and FLC control force optimized suspension parameters. A close agreement is observed between these two signals. It is observed that the FLC force of a suspension system using optimized parameters is nearly the same as that of the suspension force supplied by a passive suspension system.

The FLC active suspension system is further simulated using optimized suspension parameters as given in Table 1. It is observed that the controller force is reduced by 38% as compared to the initial FLC system. Also, VDV and RMS acceleration and maximum acceleration are reduced by 32%, 28%, and 24%, respectively, compared to the initial FLC suspension system. The optimized FLC suspension system has RMS acceleration, VDV, and maximum acceleration reduced by 62%, 61%, and 44%, respectively, compared to the initial passive suspension system. Refer to Fig. 10 for all combined plots (initial passive suspension system, initial FLC suspension system, optimized passive suspension system, and optimized FLC suspension system) and Table 2.

Frequency domain analysis is carried out to validate the performance of the initial passive, initial FLC system, optimized passive, and optimized FLC system. The optimized passive suspension system, which mimics the FLC active system, has 39.5% less amplitude compared to the initial passive suspension system at nearly 2 Hz frequency for the first peak, whereas 44.7% less amplitude at the second peak. According to frequency analysis, the fuzzy logic-controlled system has lower amplitudes of vibrations than the initial passive suspension system. Compared to all other systems, the FLC system with optimal parameters has a low amplitude of vibrations. Refer to Fig. 11 and Table 3 for more details.

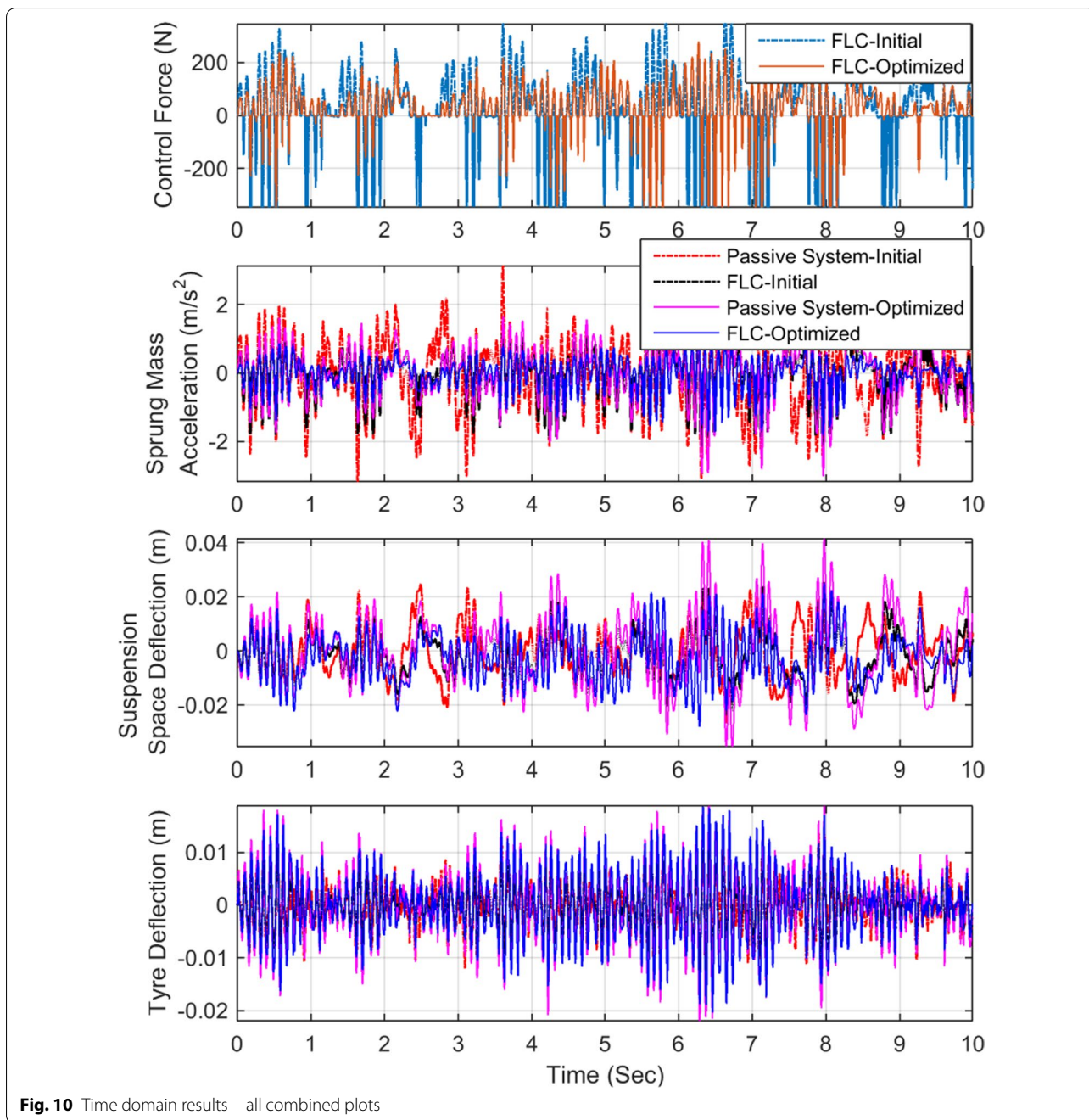


Fig. 10 Time domain results—all combined plots

Based on frequency-weighted RMS acceleration, Fig. 12 illustrates exposure levels for initial passive, initial FLC, optimized passive and optimal FLC. The time duration for NHR, PHR, and LHR limit values is shown in Table 4. Vibration exposure limits for initial passive systems are up to 2 h for NHR, up to 6 h for initial FLC systems, and 5 h and 10 h for optimized passive and optimal FLC systems, respectively. The duration of the PHR and LHR cutoff levels is also shown in Table 2.

An optimized passive suspension system mimicking the FLC active system has 150% higher potential health risk time limits. Thus, the optimized passive suspension system has an HGCZ time 1.5 times greater than the initial passive suspension system for no health risk limits. An optimized passive suspension system has a 42% higher time limit for LHR than the initial passive system, i.e., the initial passive suspension system has 42% higher chances of likely health risk. Thus, an optimized passive

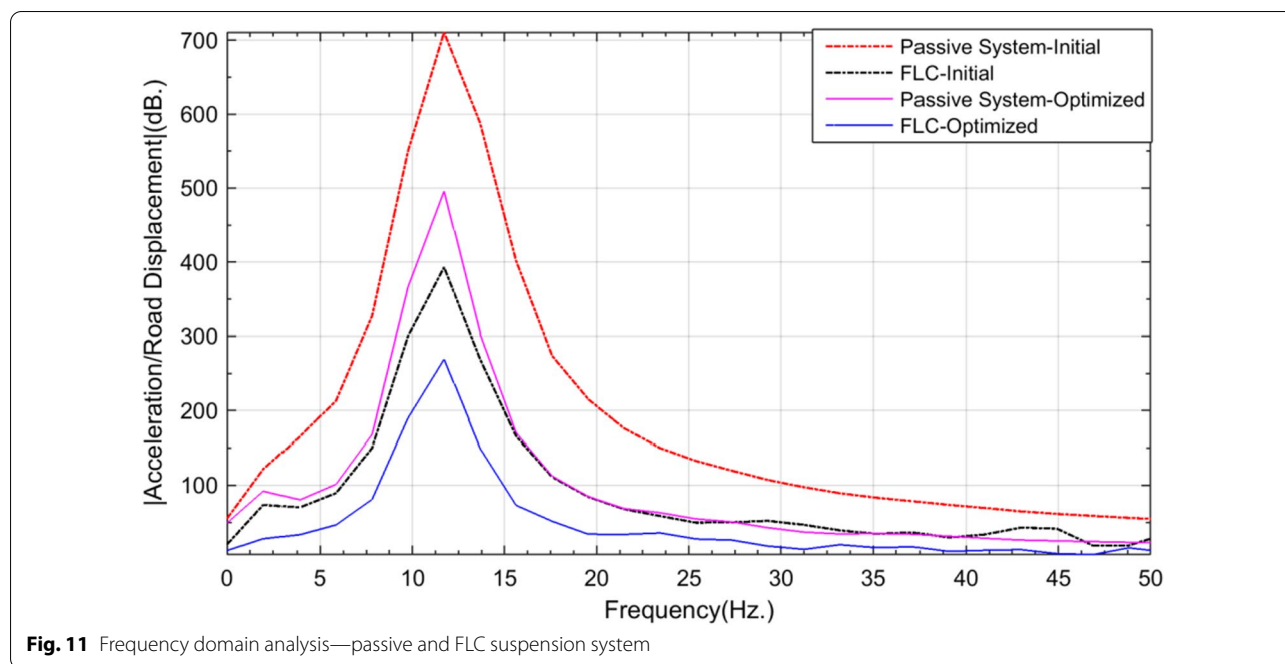


Table 3 Frequency response results—passive and FLC suspension system

Type of system	First peak		Second peak	
	Amplitude (dB)	Frequency (Hz)	Amplitude (dB)	Frequency (Hz)
Passive system-initial	121.60	1.953	710.50	11.72
FLC active system-initial	92.01	1.953	495.70	11.72
Passive system-optimized	73.53	1.953	393.10	11.72
FLC active system-optimized	27.89	1.953	269.00	11.72

system improves the ride and health criterion compared to the initial passive system.

Overall, optimized FLC shows superior limit levels, as compared to other systems, of 24 h of the ride before any potential health risk.

5 Conclusion

- The least square technique is implemented to optimize and mimic a passive suspension system as the FLC active system. The optimized passive suspension system follows and works the same way as the active suspension system.
- The optimized passive suspension system has RMS acceleration and VDV values reduced by 30% and 27%, respectively, compared to the initial passive sus-

pension system. Thus, an optimized passive suspension system improves ride comfort.

- Furthermore, optimized suspension parameters emulate the FLC active suspension system. The controller force has been lowered by 38% compared to the original FLC system. In addition, VDV and RMS acceleration and maximum acceleration are reduced by 32%, 28%, and 24%, respectively.
- In addition, due to road abnormalities, the frequency response of the optimized suspension system shows less amplitude of vibrations at the sprung mass end. The suspension systems are then examined for health levels as per ISO 2631-1, Annexure B, and it is discovered that the optimized FLC system outperforms the other systems.

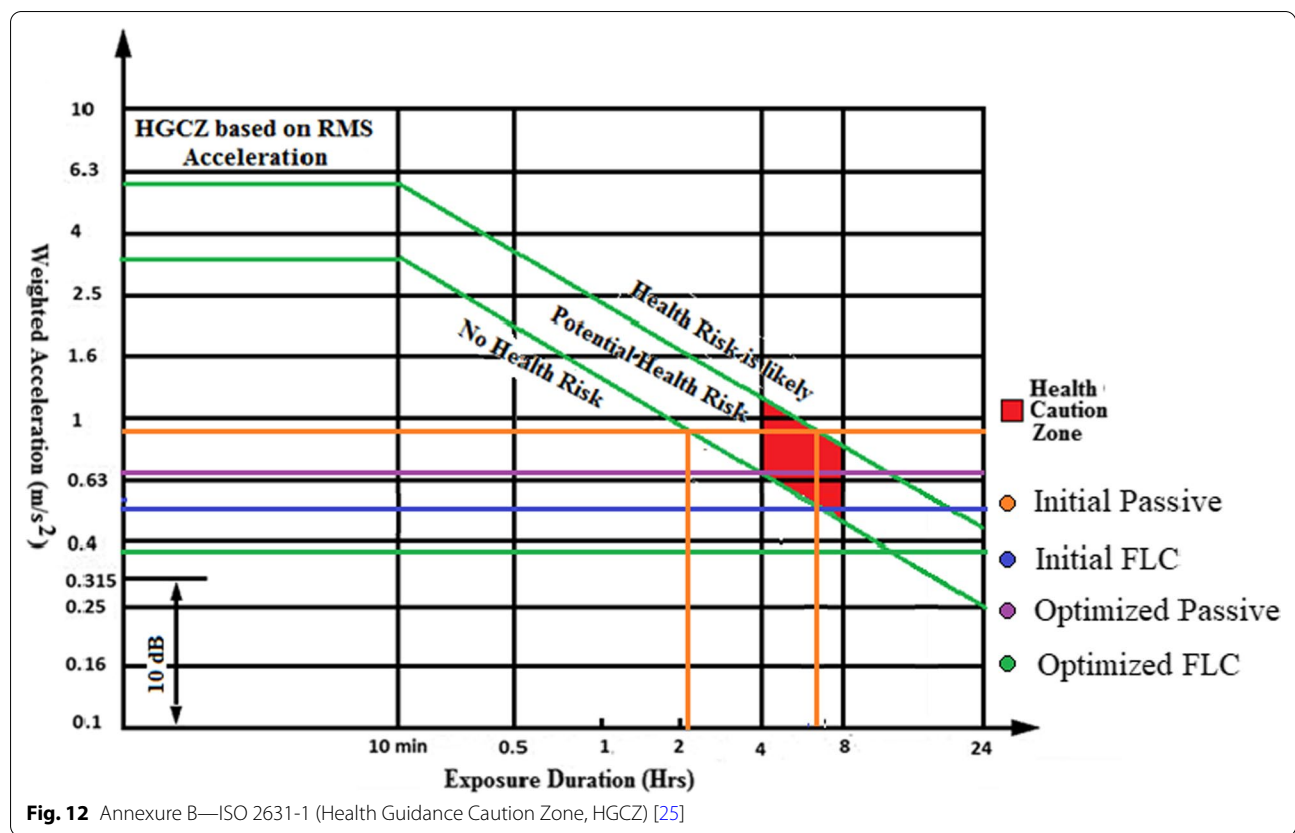


Table 4 Time limits as per Health Guidance Caution Zone (HGCZ) as per ISO—2631-1

Type of system	Frequency-weighted RMS acceleration (m/s ²)	Vibration exposure limit (h)		
		NHR	PHR	LHR
Initial passive	0.9322	2	2–7	7–24
FLC	0.5057	6	6–20	20–24
Optimized passive	0.6474	5	5–10	10–24
Optimized FLC	0.3606	10	10–24	–

Abbreviations

FLC/flc: Fuzzy logic control; VDv: Vibration dose value (m/s^{1.75}).

List of symbols

A_w: Frequency-weighted RMS acceleration (m/s²); c_g: Damping coefficient (N s/m); f: Force (N); k_s: Spring stiffness (N/m); k_{spn}: Cubic stiffness in suspension spring (N/m³); k_t: Tire stiffness (N/m); k_{tnl}: Quadratic tire stiffness (N/m²); m: Mass (kg); t: Time (s); x: Displacement (m); \dot{x} : Velocity (m/s); \ddot{x} : Acceleration (m/s²).

Subscripts

opt: Optimum; p: Passive; s: Sprung; us: Unsprung; r: Road.

Acknowledgements

First author likes to express his deep gratitude to Hon'ble Shri. Amit Kolhe Sir, Managing Trustee, Sanjivani Rural Education Society for his constant support during this work.

Author contributions

MN planned the scheme, initiated the project, and suggested the experiments; MN YB and AT developed the mathematical modeling and examined the theory validation, Authors MN, DB, VH, and RZ conducted the experiments and analyzed the empirical results. The manuscript was written through the contribution of all authors. All authors discussed the results, reviewed, and approved the final version of the manuscript. All authors read and approved the final manuscript.

Funding

The authors declare that they have no funding.

Availability of data and materials

Data sharing is not applicable to this article as no datasets were generated or analyzed during the current study.

Declarations

Ethics approval and consent to participate

Not applicable.

Consent for publication

Not applicable.

Competing interests

The authors declare that they have no known competing financial interests or personal relationships that could have appeared to influence the work reported in this paper.

Author details

¹Department of Mechanical Engineering, Sanjivani College of Engineering, Kopgaon, Savitribai Phule Pune University, Pune 423603, India. ²Department

of Mechanical Engineering, MIT Academy of Engineering (MAE), Pune, India.

³Engineering Faculty of Science, University of East Anglia, Norwich Research Park, Norwich NR47TJ, UK. ⁴Department of Mechanical Engineering, Amrutvahini College of Engineering, Sangamner, Savitribai Phule Pune University, Pune, India. ⁵Department of Mechanical Engineering, D. V. V. P. College of Engineering, Ahmednagar, Savitribai Phule Pune University, Pune, India.

Received: 2 June 2022 Accepted: 23 August 2022

Published online: 05 September 2022

References

- Fuller CR, Elloit SJ, Nelson PA (1996) Active control of vibrations. Academic Press, London
- Gobbi M, Mastinu G (2001) Analytical description and optimization of the dynamic behaviour of passively suspended road vehicles. *J Sound Vib* 245(3):457–481
- Özcan D, Sönmez Ü, Güvenç L (2013) Optimisation of the nonlinear suspension characteristics of a light commercial vehicle. *Int J Veh Technol* 2013:1–16
- Chi Z, He Y, Naterer G (2008) Design optimization of vehicle suspensions with a quarter-vehicle model. *Trans Can Soc Mech Eng* 32(2):297–312
- Gomes H (2009) A swarm optimization algorithm for optimum vehicle suspension design. In: Proceedings of 20th international congress of mechanical engineering, Brazil, pp 1–10
- Baumal A, McPhee J, Calamai P (1998) Application of genetic algorithms to the design optimization of an active vehicle suspension system. *Comput Methods Appl Mech Eng* 163:87–94
- Kuznetsov A, Mammadov M, Sultan I, Hajilarov E (2011) Optimization of a quarter-car suspension model coupled with driver biomechanical effects. *J Sound Vib* 330:2937–2946
- Gundogdu O (2007) Optimal seat and suspension design for a quarter car with driver model using genetic algorithm. *Int J Ind Ergon* 37:327–332
- Hrovat D (1997) Survey of advanced suspension developments and related optimal control applications. *Automatica* 33(10):1781–1817
- Anderson B, Moore J (1990) Optimal control—linear quadratic methods. Prentice Hall, Hoboken
- Zhen L, Luo C, Hu D (2006) Active suspension control design using a combination of LQR and backstepping. In: Proceedings of the 25th Chinese control conference, China, pp 123–125
- Nagarkar MP, Bhalerao YJ, Vikhe Patil GJ, Zaware Patil RN (2017) Multi-objective optimization of nonlinear quarter car suspension system—PID and LQR control. *Procedia Manuf* 20:420–427
- Sam YM, Osman HSO, Ghani MRA (2004) A class of proportional–integral sliding mode control with application to active suspension system. *System Control Lett* 51:217–223
- Kalaivani R, Lakshmi P, Sudhagar K (2014) Hybrid (DEBBO) fuzzy logic controller for quarter car model. In: Proceedings—UKACC international conference on control, Loughborough, UK, pp 301–306
- Taskin Y, Hacıoglu Y, Yagiz N (2007) The use of fuzzy-logic control to improve the ride comfort of vehicles. *Strojinski Vestnik J Mech Eng* 53(4):233–240
- Huang SJ, Chao CH (2000) Fuzzy logic controller for a vehicle active suspension system. *Proc Inst Mech Eng Part D J Autom Eng* 214(1):1–12
- Salem MMM, Aly AA (2009) Fuzzy control of a quarter-car suspension system. *World Acad Sci Eng Technol* 53:258–263
- Ding X, Li R, Cheng Y, Liu Q, Liu J (2019) Design of and research into a multiple-fuzzy PID suspension control system based on road recognition. *Processes* 9:2190. <https://doi.org/10.3390/pr9122190>
- Al-Awad NA (2019) Genetic algorithm control of model reduction passive quarter car suspension system. *Int J Modern Educ Comput Sci* 2:9–16. <https://doi.org/10.5815/ijmecs.2019.02.02>
- Senthilkumar P, Sivakumar K, Kanagarajan R, Kuberan S (2018) Fuzzy control of active suspension system using full car model. *Mechanika* 24(2):240–247
- Basari AA, Nawir NAA, Mohamad KA, Ng XY, Khafem AM (2018) Fuzzy logic controller for half car active suspension system. *J Telecommun Electron Comput Eng* 10(2):125–129
- Likaj R, Shala A, Bajrami X (2017) Optimal control of quarter car vehicle suspensions. *Int Sci J "Trans Motauto World"* 5:184–186
- Rajendiran S, Lakshmi P (2016) Simulation of PID and fuzzy logic controller for integrated seat suspension of a quarter car with driver model for different road profiles. *J Mech Sci Technol* 30(10):4565–4570
- Nagarkar MP, Bhalerao YJ, Vikhepatil GJ, Zawarepatil RN (2018) GA-based multi-objective optimization of active nonlinear quarter car suspension system—PID and fuzzy logic control. *Int J Mech Mater Eng* 13(1):1–20
- ISO: 2631-1 (1997) Mechanical vibration and shock—evaluation of human exposure to whole-body vibration. ISO, Geneva
- McGee C, Haroon M, Adams D, Luk Y (2005) A frequency domain technique for characterizing nonlinearities in a tire-vehicle suspension system. *J Vib Acoust* 127:61–76
- Deb K, Pratap A, Agarwal S, Meyarivan T (2002) A fast and elitist multi-objective genetic algorithm: NSGA-II. *IEEE Trans Evol Comput* 6(2):182–197. <https://doi.org/10.1109/4235.996017>
- ISO (1982) Reporting vehicle road surface irregularities. Technical Report, ISO, ISO/TC108/SC2/WG4 N57

Publisher's Note

Springer Nature remains neutral with regard to jurisdictional claims in published maps and institutional affiliations.

Submit your manuscript to a SpringerOpen® journal and benefit from:

- Convenient online submission
- Rigorous peer review
- Open access: articles freely available online
- High visibility within the field
- Retaining the copyright to your article

Submit your next manuscript at ► [springeropen.com](https://www.springeropen.com)